Multi-level decision-making strategy for preparation of proof load and failure tests

Lantsoght, Eva Olivia Leontien; Yang, Yuguang; van der Veen, Cor

DOI
10.1016/j.engstruct.2021.113672

Publication date
2022

Document Version
Final published version

Published in
Engineering Structures

Engineering Structures 252 (2022) 113672

Contents lists available at ScienceDirect

Engineering Structures

journal homepage: www.elsevier.com/locate/engstruct

Multi-level decision-making strategy for preparation of proof load and failure tests

Eva Olivia Leontien Lantsoght [a,b,*], Yuguang Yang [a], Cor van der Veen [a]

[a] Concrete Structures, Delft University of Technology, Stevinweg 1, 2628CN Delft, The Netherlands
[b] Universidad San Francisco de Quito, Diego de Robles y Pampite, Sector Cumbaya, EC 170157 Quito, Ecuador

ARTICLE INFO

Keywords:
Assessment
Bending moment
Collapse testing
Concrete bridges
Existing bridges
Failure testing
Finite element modeling
Load testing
Shear

ABSTRACT

Load testing and in some cases failure (or collapse) testing of bridges is a method to learn more about the behaviour of full-scale bridges in site conditions. Since such experiments, especially failure tests, are expensive, an extensive preparation of these tests is important. This paper addresses the question of when a bridge is a good candidate for a load test or a failure test. To answer this question, a multi-level assessment methodology is developed. The proposed method includes a decision tree that helps users decide which method should be used to reach the desired level of accuracy. These procedures are followed to carry out an assessment based on the load and resistance models and factors from the code, as well as to estimate the maximum required load in a collapse test based on average values and a single tandem. The procedures are illustrated with the case of the Nieuwklap Bridge in the province Groningen, the Netherlands. The multi-level analysis showed that testing the Nieuwklap bridge would most likely not result in a shear failure, and thus the test would not meet the goals of a collapse test in shear, which would provide valuable research insights. On a more abstract level, the result of this research is the development of a multi-level decision-making procedure that can be used to evaluate if a field test should be planned and can meet the identified goals.

1. Introduction

Three types of load tests on bridges can be distinguished: diagnostic load test, proof load tests, and failure tests [1]. Diagnostic load tests can be used to verify prior to opening if a new bridge behaves as it was designed [2], and for existing bridges diagnostic load tests can be used to update the analytical models that are used for the assessment with field measurements [3–5]. In a proof load test, the bridge is subjected to a load that corresponds to the factored live load or the factored live load combination. If the bridge can withstand this load without signs of distress, the test demonstrates that the bridge fulfils the code requirements [6,7]. In failure tests, the load is increased until irreversible damage or collapse occurs [8]. As such, failure tests are the only tests that give information about the (lower bound of the) ultimate capacity of a bridge, and can be used to study the system behaviour of bridge structures [9] or to learn about the behaviour of an entire subset of bridges [10]. Experiments on members taken from existing bridges can also give valuable information [11–13], but do not give insight in the system behavior.

Failure tests [14] and high-magnitude load tests [15,16] on concrete bridges are not routine tests. They typically fit within research projects, require the availability of a functionally obsolete bridge for testing, and are expensive. An overview of failure tests on concrete bridges from the literature is given in Table 1. As Bagge [8] pointed out, there has been little transfer of knowledge from one collapse testing project to the other, and the same mistakes are often repeated. In 28% of all the failure tests analysed by Bagge [8], a different failure mode occurred during the test than expected. This observation highlights the importance of an extensive preparation of bridge tests.

A subset of bridges that is the topic of research in the Netherlands are the reinforced concrete slab bridges [17]. Upon assessment, these bridges often rate insufficiently for shear, whereas upon inspection no signs of distress are observed [18]. This discrepancy is explained by the fact that according to the governing code NEN-EN 1992–1-1:2005 [19] the shear capacity is calculated as the beam shear capacity. The expression used to determine the beam shear capacity is an empirical expression derived from a statistical analysis of shear tests on beams [20,21]. The majority of the beams in the database [22] used to derive the empirical expression are heavily reinforced, small and slender beams

* Corresponding author at: Concrete Structures, Delft University of Technology, Stevinweg 1, 2628CN Delft, The Netherlands.
E-mail addresses: E.O.L.Lantsoght@tudelft.nl, elantsoght@usfq.edu.ec (E.O.L. Lantsoght), Yuguang.Yang@tudelft.nl (Y. Yang), C.vanderveen@tudelft.nl (C. van der Veen).

https://doi.org/10.1016/j.engstruct.2021.113672
Received 20 July 2021; Received in revised form 20 October 2021; Accepted 26 November 2021
Available online 5 December 2021

Nomenclature

a_v	clear shear span (face-to-face distance between the load and the support)
b	width
d_l	effective depth to longitudinal reinforcement
f_{ck}	characteristic concrete cylinder compressive strength
f_{cm}	average concrete compressive strength determined on core samples
$f_{cm,cylinder}$	average concrete cylinder compressive strength
f_{tm}	mean tensile strength of steel
f_{yd}	design yield strength of steel
f_{yk}	characteristic yield strength of steel
f_{ym}	mean yield strength of steel
k	size effect factor
m_{Ed}	design bending moment per meter width under factored load combination
m_E	mean bending moment per meter width under load combination applied in test
$m_{Rd,c}$	design bending moment capacity
$m_{R,c}$	mean bending moment capacity
m_y	mean yielding moment of the cross-section determined by yielding of the tension steel
m_u	mean ultimate bending moment capacity determined by crushing of the concrete
v_{Ed}	design shear stress under factored load combination
$v_{Ed,x}$	design longitudinal shear stress under factored load combation
v_E	mean shear stress under load combination applied in test
v_{min}	lower bound of the design shear capacity
$v_{Rd,c}$	design shear capacity
$v_{R,c}$	mean shear capacity
A_s	area of reinforcement steel
$C_{Rd,c}$	factor to determine shear capacity
E	factored load effect
$P_{bending}$	maximum load in test that is expected to cause a bending moment failure
P_{shear}	maximum load in test that is expected to cause a shear failure
$P_{yielding}$	maximum load in test that is expected to cause yielding of the reinforcement steel
R	factored resistance
$UC_{bending}$	Unity Check for bending moment
UC_{shear}	Unity Check for shear
γ_c	material factor for concrete
γ_{DC}	load factor for selfweight
γ_{DW}	load factor for superimposed dead load
γ_{LL}	load factor for live load
ρ_{ly}	longitudinal reinforcement percentage

Table 1
Overview of failure tests on concrete bridges from the literature.

Reference	Bridge name	Bridge type	Failure mode
[26]	Barr Creek	reinforced concrete slab bridge	Bending moment
[27,28]	Niobrara River	reinforced concrete slab bridge	Bending moment
[29,30]	Batavia bridge	reinforced concrete slab bridge	Punching
[31]	ND-18	reinforced concrete slab bridge	Bending moment
[32]	LIC-310–0396	box girder bridge	Bending moment
[33–35]	Kiruna bridge	prestressed girder bridge	Punching + shear
[36–40]	Örnsköldsvik bridge	through girder bridge (strengthened)	Shear
[41]	East Meng Jiang Nu	prestressed hollow core slabs	Bending moment
[42–44]	Nanping	tub girder bridge	Bending moment
[45]	Stony Creek	concrete deck on steel girders	Yielding of steel girders
[46]	Huning Expressway	box girder bridge	Bending moment
[15]	Rosmosevej	open T-beams	Bending moment
[10,47–53]	Ruytenschildt Bridge	reinforced concrete slab bridge	Bending moment
[9,54]	Vechtbridge	prestressed girder bridge	Shear + punching
[55–58]	Hammelburg Bridge	prestressed girder bridge (with saw cut)	Shear

tested in three- or four-point bending. In slabs, transverse redistribution leads to a higher capacity, not included in the beam shear capacity expression, and traditionally not considered in the assessment [23,24]. In addition. because of the large inherent uncertainty on shear failure, design equations lead to a lower shear resistances compared to ductile failure modes [20,25].

For the assessment of reinforced concrete slab bridges, a framework using different Levels of Approximation has been developed over the past years in the Netherlands [59]. The philosophy of using Levels of Approximation was first introduced in the 2010 edition of the *fib* Model Code [60], see Fig. 1. For increasing Levels of Approximation, the accuracy of the prediction increases, as well as the computational time and effort. Other applications of using multi-level assessment methods include an application to deck slabs [61,62], as well as the approach for assessment used in France [63], Switzerland [64,65], Austria [11], Germany [66,67], and Sweden [68]. Decision-making strategies for bridge structures are discussed in [69] from a life-cycle cost point of view, and these strategies focus increasingly on minimizing the use of resources and a reduction of the carbon footprint, which often translates into strategies for extending the service life of existing infrastructure.

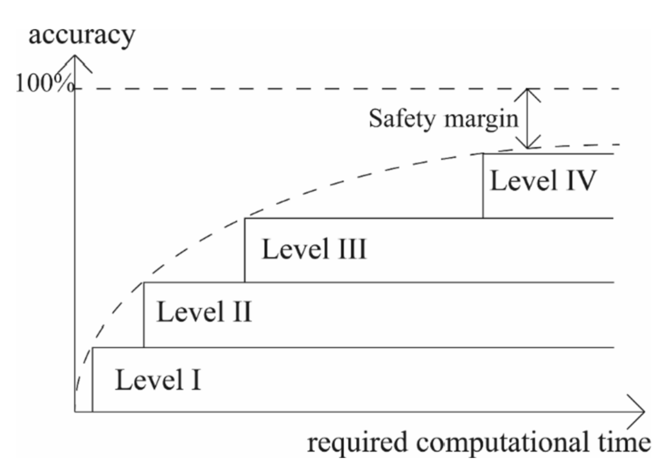

Fig. 1. Principle of Levels of Approximation. Figure reused from [59] with permission from Wiley.

2. Proposed multi-level assessment and decision-making procedures

For failure tests, extensive preparations are recommended (also pointed out by Bagge [8]). The preparations [70] are necessary to evaluate the failure mode, and to define the goals and verify if the proposed test and test methods can be used to meet these goals. Failure tests are expensive and time-consuming, so that a thorough preparation is key. This paper proposes a multi-level methodology that can be followed when evaluating the feasibility of a failure test. The proposed procedures are illustrated for the case of the Nieuwklap bridge, a reinforced concrete slab bridge in the province of Groningen in the Netherlands.

Fig. 2 shows the presented method in the form of a flowchart. The first step in the procedure is to clearly define the goals of the collapse test, and to evaluate if the available information is sufficient. If all required information is available or has been collected or measured, a double approach is followed.

On one hand, a ***multi-level assessment procedure*** is carried out (see Fig. 3), to carry out the assessment of the bridge according to the code regulations at multiple levels. All calculations use load and resistance factors. The results of this part of the analysis are the Unity Checks and the failure mode according to assessment procedures. The Unity Check is defined as the ratio of the factored load effect to the design capacity, UC $= E/R$. If the Unity Check UC ≤ 1, the considered cross-section fulfils the code requirements for the considered safety level. Note that in the Netherlands for existing structures, different safety levels with different associated reliability indices are defined in the code NEN 8700:2011 [71] and the guidelines for the assessment of bridges "Richtlijnen Beoordeling Kunstwerken" (RBK) [72], see Table 2.

The multi-level assessment method focuses in detail on the failure mode, as Bagge [8] noted that in a number of reported collapse tests, the failure mode in the field did not correspond with the predicted failure mode. In particular, information about the failure mode can lead to the step of "structure may not be interesting for testing". Flexural capacity is rather straightforward to determine, so bridges that are identified as flexure-critical may not be interesting for a collapse test. Other reasons to identify that the bridge may not be interesting for testing are, for example, a structurally determinate system without the ability to redistribute load, so that limited information about the system behavior can be obtained.

Parts of the steps in this procedure may already be available in the documentation of the bridge. The reader should note that a preliminary assessment may be available, and such a preliminary assessment may have resulted in the interest of the bridge owner in testing the bridge. Depending on the level of detail involved in the preliminary assessment, (part of) this information may be used for the multi-level assessment procedure. However, for the preparation of the test, it is good practice to develop at least a linear finite element model. When a non-linear finite element model is used, a safety format should be chosen and applied, or several safety formats can be compared [73–75].

On the other hand, a ***multi-level prediction procedure*** is carried out (see Fig. 4). All calculations use mean material properties and all load and resistance factors are taken as equal to one. The applied load during the test replaces the live load model. The results of this part of the analysis are the maximum load that is expected to cause failure, and the expected failure mode, which can change as different positions for the test load or different test load configurations are explored. The nonlinear finite element models here have as their goal to predict the behaviour of the bridge during the test as accurately as possible. When there are uncertainties regarding parameters, the effect of varying these parameters on the expected outcome during the test can be evaluated. Note that the capacity models from the code may be overly conservative, such as for the case of the shear capacity of reinforced concrete slab bridges [77] or post-tensioned girders with low amounts of stirrups [78]. In such cases, Level of Approximation III may be necessary to get a better estimate of the capacity and failure mode, or simplified calculation methods proposed in the literature may be used to replace the capacity expressions recommended by the governing codes.

The flowcharts in Fig. 3 and Fig. 4 show the application of the concepts to a case of a bridge where the goal of the test is to cause a shear failure. As such, checks to see if shear failure would occur before flexural failure are included in the decision-making strategy. If the test is prepared for a different objective, the user should check the specified objective in those steps.

With the information from the multi-level assessment and prediction calculations, the goals of the test have to be evaluated. The test goal can follow from an initial assessment, which may indicate insufficient resistance in bending, shear, or another failure mode, or it can follow from a specific goal as defined by the bridge owner. If the considered bridge cannot be used to meet the goals of the test, it is not recommended to pursue a test on the bridge. If the considered bridge is a good candidate to meet the goals, the test engineers can proceed with the practicalities of the test. The load positions, loading protocols, and maximum load are determined together with the sensor plan. After taking these decisions, the test engineers and safety engineers need to evaluate if it is possible to carry out all activities on site safely. If there are concerns regarding the safety of the personnel involved and/or the traveling public, then it is not recommended to pursue a test on the bridge, as shown as well in Fig. 2.

Since collapse tests, as well as proof load tests, are costly and time-consuming, a careful preparation is necessary. A bridge owner may want to select immediately the most refined calculation method to prepare a test, but our approach here shows that this choice may not always be the wisest for two reasons: 1) a faster and lower level approach may already sufficiently answer the questions about whether the test would be able to meet the objectives or not, so that more costly calculation procedures become unnecessary, and 2) the lower level calculations can be used to explore the effect of different test choices, such as different loading positions, which can serve to prepare for the higher level calculations, and so that the number of higher level calculations necessary can be optimized.

3. Description of the Nieuwklap bridge

3.1. History and general information

The Nieuwklap Bridge, see Fig. 5, is a reinforced concrete slab bridge with 7 spans, designed in 1937 and built in 1941. The original design drawings and calculations considered the option of a bridge with five spans and the option of a bridge with seven spans. The documentation of the option of a bridge with five spans is complete with all drawings and the original hand calculations, whereas not all information about the option with seven spans is available in the archives. The soil profiles resulting from sampling from 1937 are also available, which was important for the assessment of the substructure, as well as the risk of substructure failure when a high magnitude load is applied to the bridge.

The Nieuwklap Bridge is part of the Friesestraatweg road between Aduarderzijl and Leegkerk and crosses the river Aduarderdiep. The Friesestraatweg connects Groningen and Leeuwarden. In 2014 the owner decided to demolish the Nieuwklap Bridge in September 2018.

The most recent inspection is from October 5th 2015 [79]. Corrosion is observed on the guide rails, handrails, sheet piles, steel supports, and sidewalk. The bottom of the superstructure slab shows damage, see Fig. 6. Similar damage is observed at the supports and on the piers.

3.2. Geometry

The Nieuwklap Bridge is a seven-span reinforced concrete slab bridge of 101 m length in total. The end spans are 11.20 m long and the central spans are 14.14 m long. The skewness of the bridge is 8°. Fig. 7 shows the numbering of the spans and supports and the longitudinal

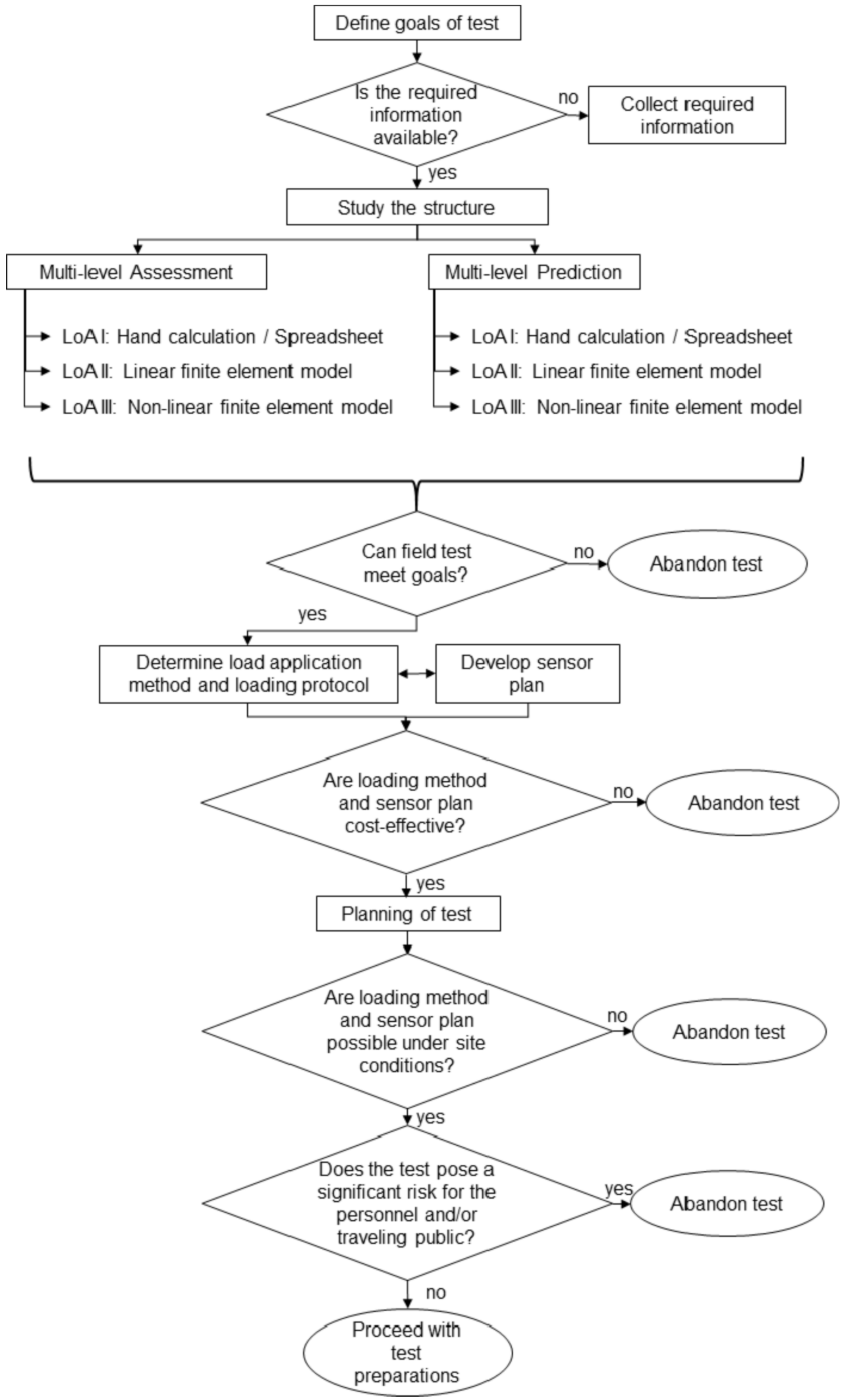

Fig. 2. Proposed multi-level assessment and decision-making approach for preparation stage of field tests.

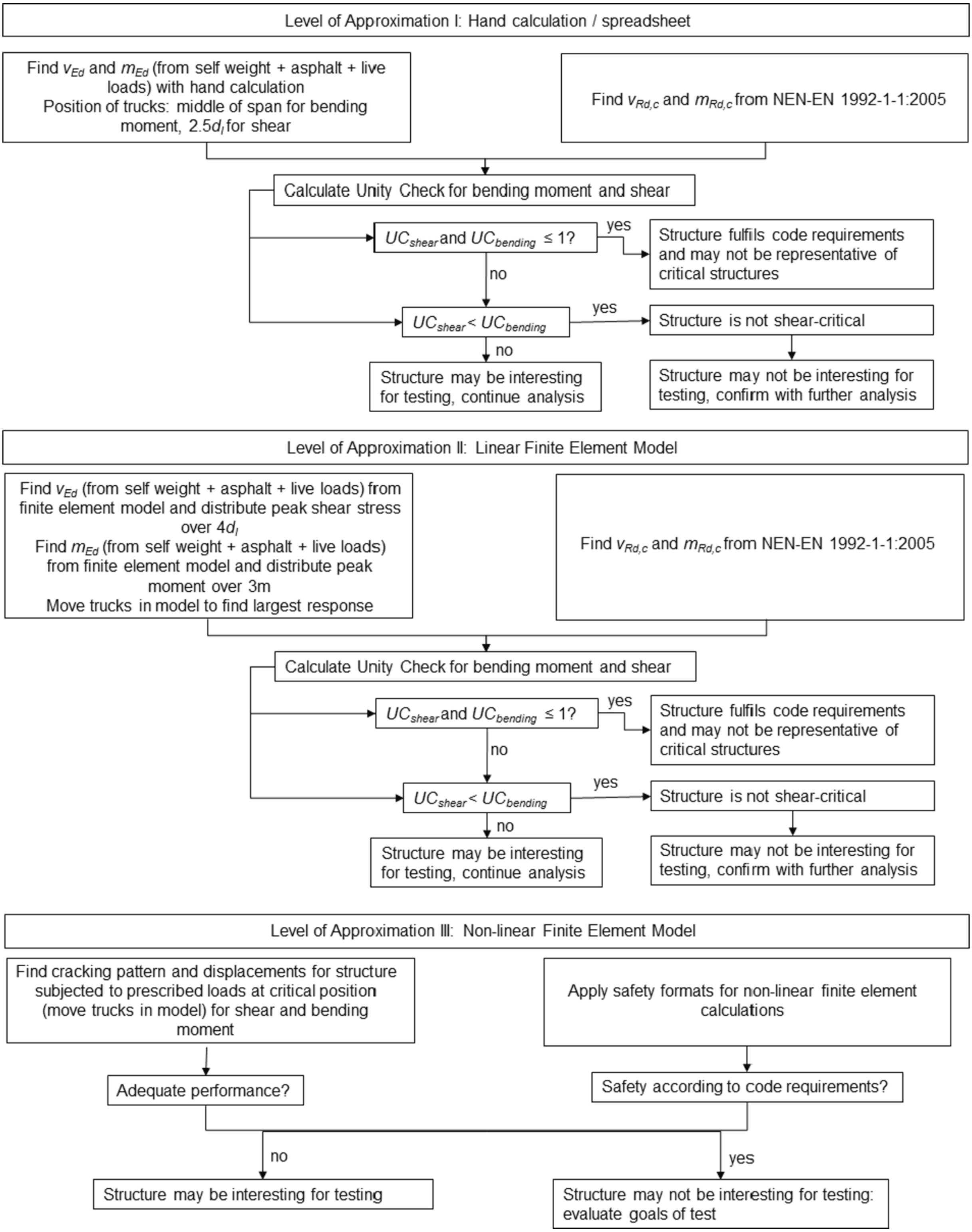

Fig. 3. Detail of multi-level assessment from Fig. 2.

view of the bridge. The total width is 14.31 m. The width of the carriageway is 7.25 m, the width of the sidewalk and edge beam is 1.00 m, and the width of the bike lane is 2.53 m. Fig. 8 shows the cross-section of the Nieuwklap Bridge.

3.3. Material properties

For the superstructure, a concrete with 400 kg cement per m^3 was used. In spans 1, 2, 6, and 7 core samples are taken. The samples from spans 6 and 7 are taken from the carriageway, whereas the samples from spans 1 and 2 from the bike lane. The samples from spans 6 and 7 are used to determine the concrete compressive strength, and the samples from spans 1 and 2 are used to determine the tensile strength of the concrete. The average compressive strength of the cores is f_{cm} = 83.29 MPa with a standard deviation of 7.79 MPa and a coefficient of variation of 9.3% determined from 7 cores. The corresponding average cylinder

Table 2
Considered safety levels governing in the Netherlands [72,76].

Safety level	β	Ref period	γ_{DC}	γ_{DW}	γ_{LL}
Eurocode Ultimate Limit State	4.3	100 years	1.25	1.35	1.50
RBK Design	4.3	100 years	1.25	1.25	1.50
RBK Reconstruction	3.6	30 years	1.15	1.15	1.30
RBK Usage	3.3	30 years	1.15	1.15	1.25
RBK Disapproval	3.1	15 years	1.10	1.10	1.25
Eurocode Serviceability Limit State	1.5	50 years	1.00	1.00	1.00

compressive strength is then $f_{cm,cylinder}$ = 68.30 MPa using the conversion factors recommended in the Netherlands [80] and the characteristic compressive strength is f_{ck} = 60.30 MPa. The average spilling tensile strength of the concrete is 5.15 MPa (standard deviation = 0.61 MPa, coefficient of variation = 11.9% based on 7 cores). The relation between tensile and compressive strength of the concrete is as expected. In some existing bridges, low tensile strengths are found [81], which raises concerns for the shear capacity. For the Nieuwklap Bridge, that is not the case.

The maximum size of the aggregates was about 31.5 mm. In some historical bridges, even larger sizes of coarse aggregates were used, but the observations on the core samples show that this is not the case for the Nieuwklap Bridge.

No information is available about the reinforcement steel, and no samples of the reinforcement steel have been tested yet. Given the time period of construction, it is expected that either QR22 or QR24 steel was

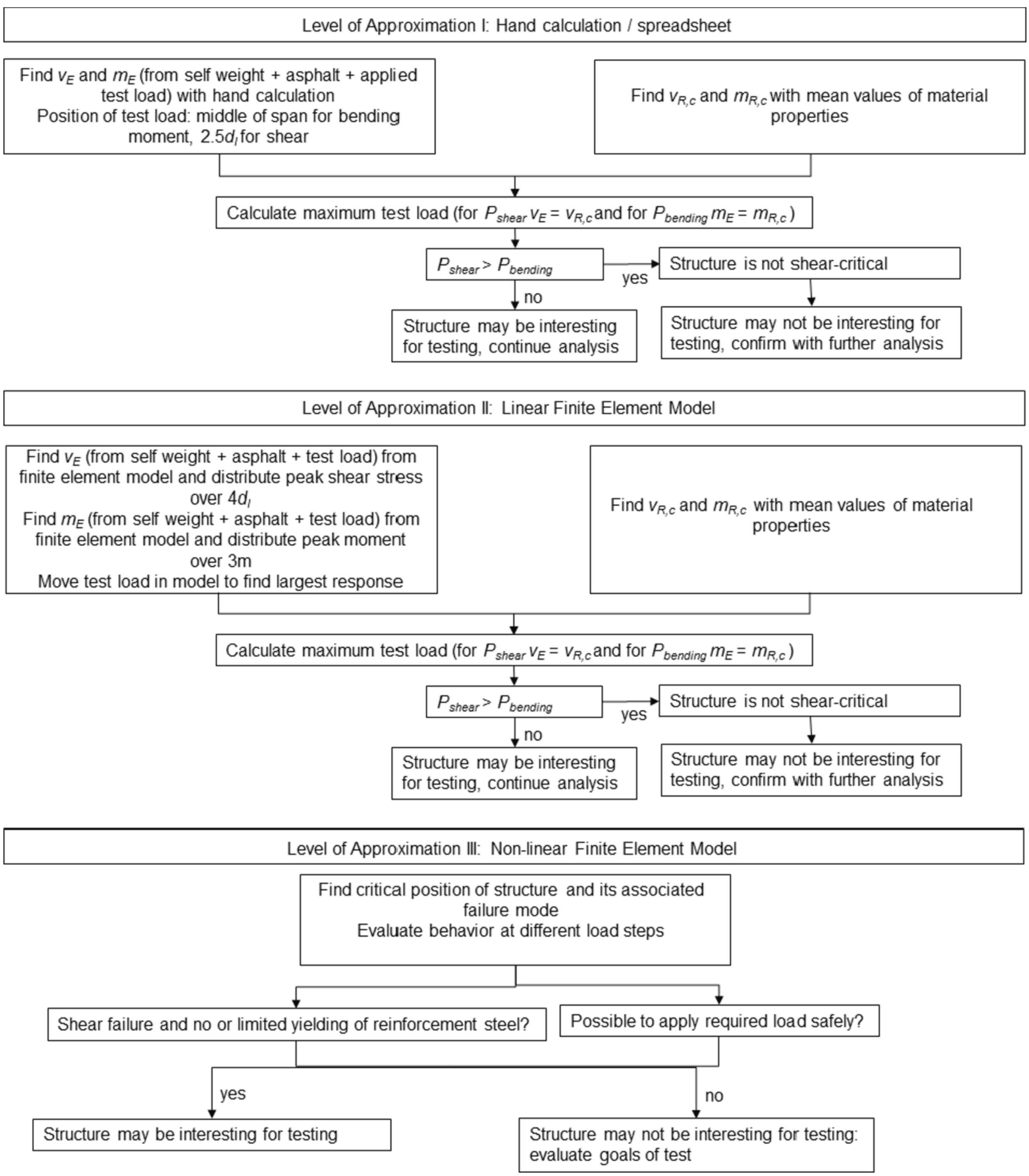

Fig. 4. Detail of multi-level prediction approach from Fig. 2.

Fig. 5. Google Maps view of Nieuwklap Bridge.

Fig. 6. Damage to the bottom of the reinforced concrete slab.

used. The properties of these steel types are given in Table 3. For the calculations, QR22 is assumed, and for a few cases, QR24 is studied as a variation. The properties of historic steel qualities are prescribed in the Dutch Guidelines for the Assessment of Bridges (RBK – Richtlijnen Beoordeling Kunstwerken [82]). A top view of the reinforcement in spans 1 and 2 is shown in Fig. 9, with the section at midspan in Fig. 10, the section over the support in Fig. 11, and a section in the longitudinal direction showing the detailing of the bars in Fig. 12. The bottom reinforcement in span 1 consists of following layers: 30 ϕ 25 mm, 14 ϕ 25 mm, 32 ϕ 25 mm, and 16 ϕ 25 mm. The resulting reinforcement area is 6229 mm^2/m and the reinforcement ratio is 1.06%. In span 2, the bottom reinforcement consists of 30 ϕ 25 mm, 32 ϕ 25 mm, and 30 ϕ 25 mm, so that the area is 6229 mm^2/m and the reinforcement ratio 1.08%. The top reinforcement over the support consists of the following layers of steel: 34 ϕ 25 mm, 34 ϕ 25 mm, 30 ϕ 25 mm, and 36 ϕ 25 mm. The resulting reinforcement area is 9073 mm^2/m and he reinforcement ratio is 1.5%. Further details of the plans can be found in the report of this study [83].

3.4. Test objectives

The Nieuwklap bridge is a reinforced concrete slab bridge which became available for a possible collapse test, as the bridge was scheduled for replacement. Many reinforced concrete slab bridges in the Netherlands are found to be shear-critical upon assessment [84]. Past laboratory research [77,85] focused on identifying the sources of additional capacity in slabs failing in shear under concentrated loads as compared to beams. However, the findings had not yet been confirmed with a failure test of an actual reinforced concrete slab bridge in shear. As such, a collapse test in shear on the Nieuwklap bridge was interesting from a research perspective, and to improve the methods of assessment of the shear-critical reinforced concrete slab bridges in the Netherlands. In addition, all laboratory tests in the past were carried out on straight slabs, and there were some concerns with regard to the shear capacity of skewed slabs. In skewed slabs, stresses are concentrated in the obtuse corner and the transverse distribution found in straight slabs may not be valid anymore.

4. Numerical model

For the Level of Approximation II calculations (assessment and prediction), a linear finite element model is developed in Scia Engineer 17 [86]. The variable thickness (see Fig. 9c and d) is simplified to a constant thickness of 650 mm. Ideal support conditions are assumed. Fig. 13 shows an overview of the model. The element size is 200 mm, so that the resulting mesh contains 16,300 nodes and 15,925 2D elements. The element type is Mindlin element, which includes the shear force deformation, and is the standard element for plates in Scia Engineer.

The carriageway width is 7.25 m, which results in 2 notional lanes of 3 m wide and a remaining area. The loads in the model are the self-weight (determined directly by the model), the superimposed dead load from the asphalt (assuming a layer of 12 cm), and the live loads. The first lane with the heavier loads is assumed in the obtuse corner [87,88], which is the critical situation for shear.

For the assessment calculations, the live loads of NEN-EN 1991–2:2003 [89] Load Model 1 are used. This Load Model consist of a uniformly distributed load of 9 kN/m^2 in the first lane, a uniformly distributed load of 2.5 kN/m^2 in the second lane, a pedestrian load of 5 kN/m^2, a distributed load on the remaining area of 2.5 kN/m^2, a tandem with two axles of 300 kN in the first lane, and a tandem with two axles of 200 kN in the second lane. The wheel prints of the tandem are 400 mm $\times$ 400 mm, which is distributed under 45° vertically to the centerline of the slab because a linear finite element model is used. Therefore, a wheel print of 1050 mm $\times$ 1050 mm is used in the model. All details of the calculations are given in the background report [83].

For the prediction calculations, the live load is replaced by a single proof load tandem for which the maximum load is sought. The position of the proof load tandem is taken as the position of the first design tandem in the configuration of the design tandem that results in the largest load effect (i.e., the largest bending moment). The load factors are taken as equal to 1. The maximum load on the proof load tandem is determined for which the sectional moment reaches the bending moment capacity, and for which the sectional shear reaches the shear capacity.

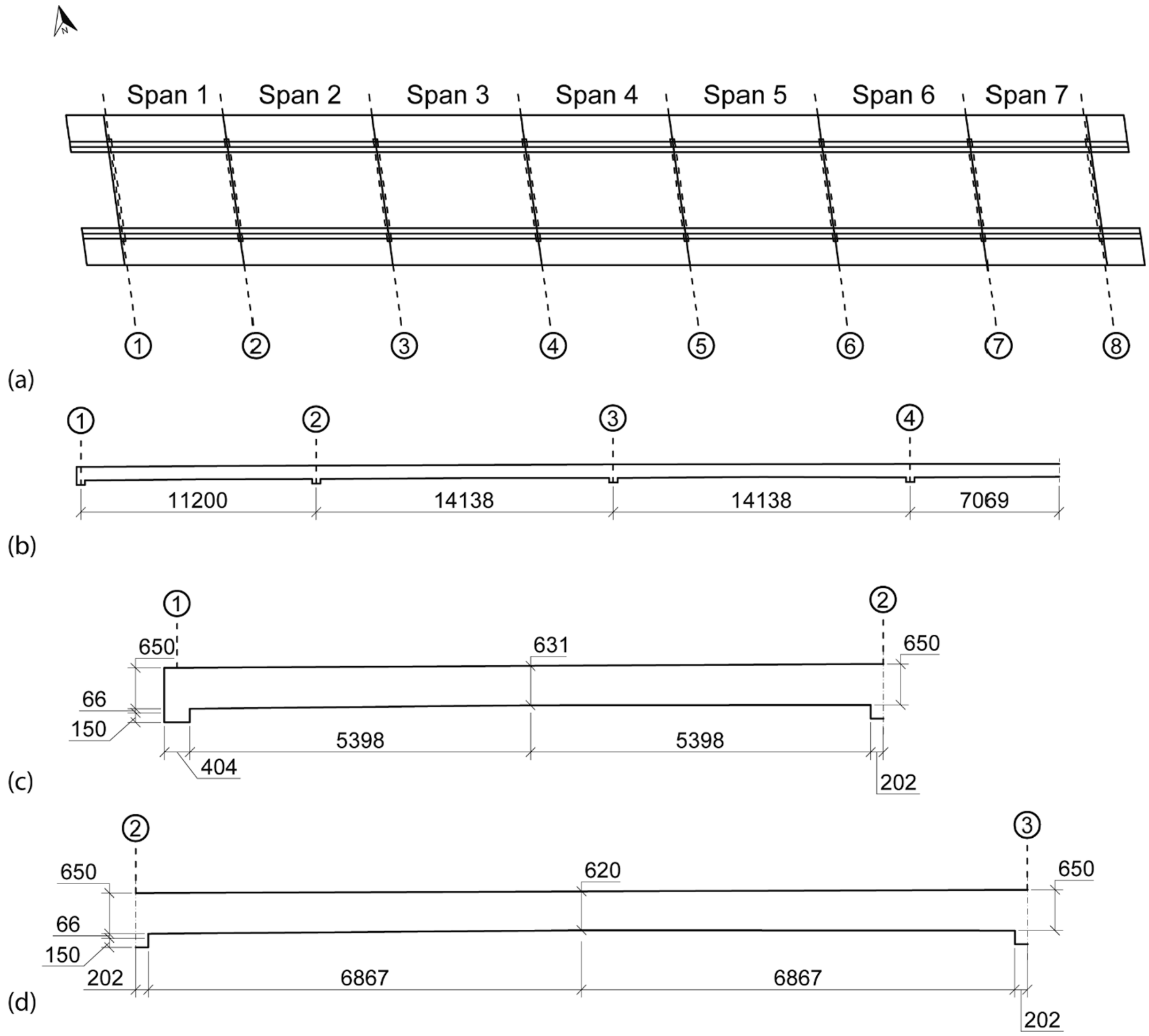

Fig. 7. Geometry of Nieuwklap Bridge: (a) top view with numbering of spans and supports, (b) longitudinal view of symmetric half of bridge, (c) detail of longitudinal view for span 1, (d) detail of longitudinal view of span 2. Units: mm.

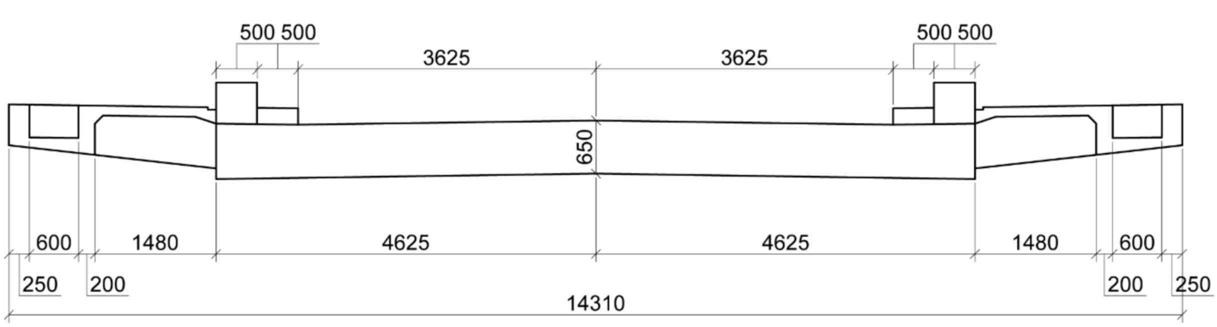

Fig. 8. Cross-sectional view of the Nieuwklap Bridge. Units: mm.

Table 3
Properties of QR22 and QR24 steel.

	QR22	QR24
f_{yd} (MPa)	191	209
f_{yk} (MPa)	220	240
f_{ym} (MPa)	242	264
f_{tm} (MPa)	330	360

5. Multi-level assessment of the Nieuwklap bridge

5.1. Level of Approximation I

The multi-level assessment and prediction models are used to study if a collapse test for shear can be carried out in spans 1 and/or 2 of the Nieuwklap bridge. These spans are selected, as they are not over water, which would make instrumentation more practical. For Level of

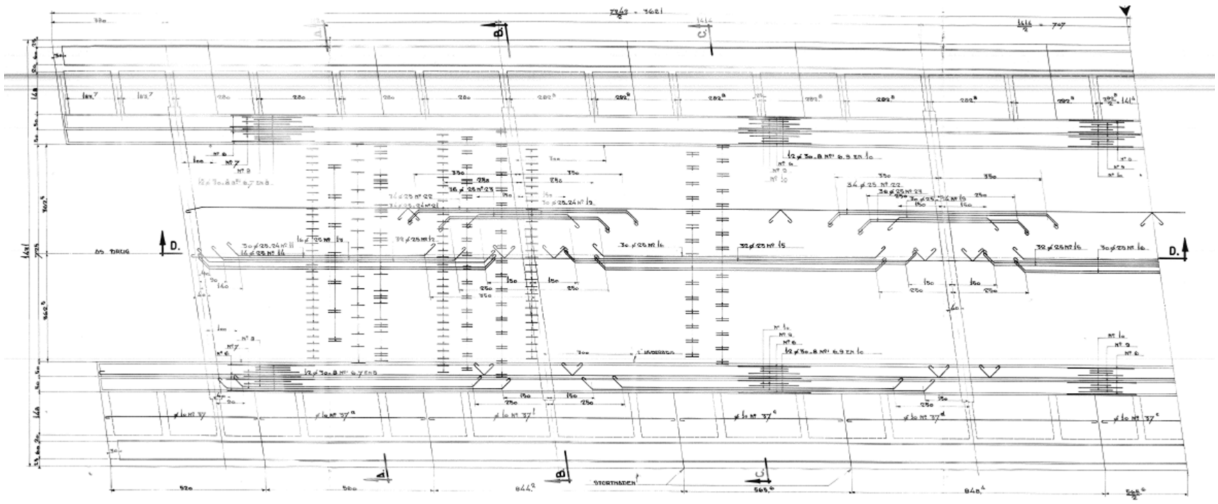

Fig. 9. Top view of longitudinal reinforcement for spans 1, 2, and half of span 3. Dimensions in cm, except for bar diameters in mm.

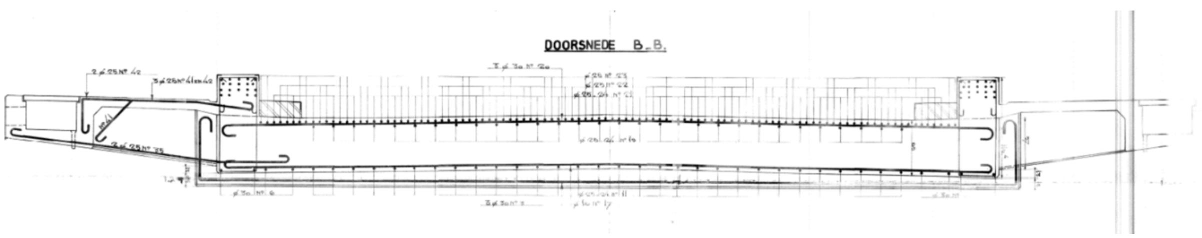

Fig. 10. Cross-section in span. Dimensions in cm, except for bar diameters in mm.

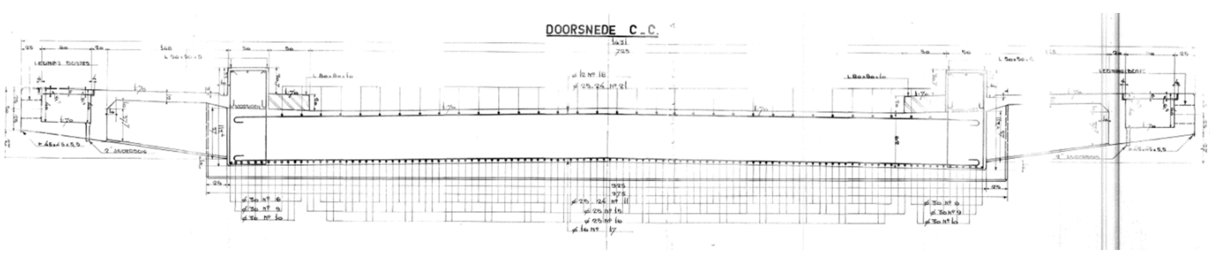

Fig. 11. Cross-section over the support. Dimensions in cm, except for bar diameters in mm.

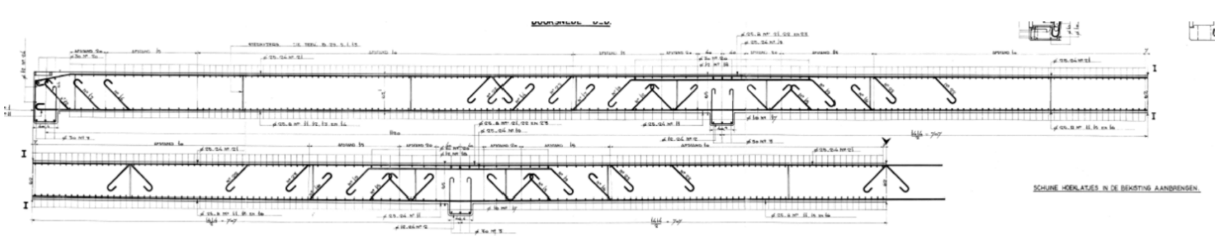

Fig. 12. Longitudinal view of reinforcement showing hooks at the end of the longitudinal bars. Dimensions in cm, except for bar diameters in mm.

Approximation I, hand calculations or simple spreadsheets are used for the assessment of reinforced concrete slab bridges [90]. An example of such a simple spreadsheet approach is the Quick Scan [91], which was used in the Netherlands for the shear assessment of reinforced concrete slabs until 2017. Since for the preparation of field tests on bridges [92], linear finite element models are recommended, only the Unity Check for shear is determined for LoA I with the existing Quick Scan sheet.

To determine the maximum sectional shear, the critical position is taken by placing the first design tandem at a face-to-face distance to the support of 2.5 d_l, with d_l the effective depth to the longitudinal reinforcement [17], which for the geometry of the Nieuwklap Bridge becomes $a_v = 1.5$ m. The second design tandem is placed in such a way that the effective width just reaches the edge of the slab, $a_v = 1.975$ m. Note that this critical position was derived for straight slabs with a constant thickness and constant reinforcement. For the Nieuwklap Bridge, bent-up bars are used in the shear-critical region, which may alter the critical position of the load as these bars may increase the shear capacity. From Fig. 12, the shape of these bent-up bars can be seen. These bent-up

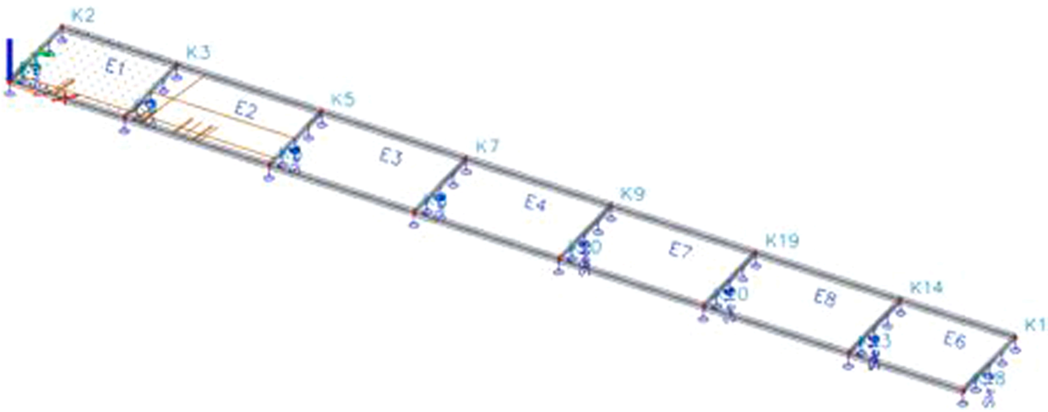

Fig. 13. Overview of linear finite element model.

bars differ from the regular bent-up bars between the top and bottom reinforcement. Here, they are large hooks, which are not anchored to the other layer of reinforcement, so that their efficiency as shear reinforcement can be subject to discussion.

To find the maximum sectional shear, vertical load distribution of the wheel prints under 45°to the center of the cross-section is assumed. In addition, to find the maximum sectional shear at the face of the support, a 45-degree horizontal load distribution is assumed from the far side of each axle of the design tandem to the face of the support. This horizontal load distribution determines the effective width in shear, over which the applied concentrated load (axles of the design tandem) is distributed [93,94].

The shear capacity is determined with $v_{Rd,c}$ according to NEN-EN 1992–1-1:2005 [19] and v_{min} as recommended by Walraven [95]:

$$v_{Rd,c} = C_{Rd,c}k\left(100\rho_{ly}f_{ck}\right)^{1/3} \geqslant v_{min} = \frac{1.08k^{3/2}f_{ck}^{1/2}}{f_{yk}^{1/2}} \tag{1}$$

The factor $C_{Rd,c}$ equals $0.18/\gamma_c$ with $\gamma_c = 1.5$. The material properties are determined with f_{ck} the concrete cylinder compressive strength and f_{yk} the characteristic yield strength of the steel. The size effect factor k is determined as:

$$k = 1 + \sqrt{\frac{200\text{mm}}{d_l}} \leqslant 2 \tag{2}$$

The reinforcement ratio is determined as:

$$\rho_{ly} = \frac{A_s}{bd_l} \tag{3}$$

with A_s the area of the longitudinal reinforcement steel, b the width of the cross-section, and d_l the effective depth to the longitudinal reinforcement. For span 1, $A_s = 6229$ mm^2/m and $d_l = 586$ mm. For span 2, $A_s = 6229$ mm^2/m and $d_l = 575$ mm. For the initial assessment, $f_{ck} = 45$ MPa [96] is assumed and QR 22 steel is assumed. The shear capacity is then 571 kN/m in span 1 and 563 kN/m in span 2.

5.2. Level of Approximation II

To determine the maximum sectional moment, the critical position of the design tandems is sought by moving the tandems in their respective lanes. For span 1, the critical position for bending moment is found with the face of the tandem at 4.148 m from support 1, and for span 2 at 17.748 m from support 1. The sectional moment is averaged over a width of 3 m [97]. The bending moment capacity is determined by using a rectangular stress block, conservatively assuming $f_{cd} = 30$ MPa [96] and QR 22 steel. At support 2, $A_s = 9073$ mm^2/m and $d_l = 605$ mm. For span 1, $m_{Rd,c} = 671$ kNm/m. For span 2, $m_{Rd,c} = 658$ kNm/m. Over support 2, $m_{Rd,c} = 986$ kNm/m. Table 4 and Table 5 show the Unity Checks for bending moment in span 1 and span 2, respectively. Since the results of RBK Disapproval and RBK Usage are very similar, only RBK Usage is included in Table 5. From these results, it can be seen that for the RBK Design load combination in span 2, the UC is slightly larger than 1.

For the shear assessment, the same critical positions and the same shear capacity are used as for LoA I. The peak shear stress is averaged over a distance 4 d_l in the transverse direction [98]. The results are given in Table 6 and Table 7 for spans 1 and 2 respectively. Comparing the results of the Unity Checks for bending moment and shear (Table 4 with Table 6 for span 1, and Table 5 with Table 7 for span 2) shows that the Nieuwklap Bridge is not shear-critical. Comparing the results for Levels of Approximation I and II in Table 6 and Table 7 shows that LoA I is more conservative (larger UC) than LoA II, as expected. From these assessment results, it can be concluded that the Nieuwklap Bridge is not representative of the shear-critical reinforced concrete slab bridges in the Netherlands. However, the second step in the multi-level decision-

Table 4
Resulting Unity Checks for different Levels of Approximation for bending moment, span 1.

	LoA II m_{Ed} (kNm/m)	$m_{Rd,c}$ (kNm/m)	UC
RBK Disapproval	564.10	671.41	0.84
RBK Usage	572.31	671.41	0.85
RBK Reconstruction	587.65	671.41	0.88
RBK Design	655.44	671.41	0.98

Table 5
Resulting Unity Checks for different Levels of Approximation for bending moment, span 2.

	LoA II m_{Ed} (kNm/m)	$m_{Rd,c}$ (kNm/m)	UC
RBK Usage	582.49	658.58	0.88
RBK Reconstruction	598.23	658.58	0.91
RBK Design	677.61	658.58	1.03

Table 6
Resulting Unity Checks for different Levels of Approximation for shear, span 1.

	LoA I $v_{Ed,x}$ (kN/m)	$v_{Rd,c}$ (kN/m)	UC	LoA II $v_{Ed,x}$ (kN/m)	UC
RBK Usage	258.08	570.73	0.45	243.14	0.43
RBK Reconstruction	264.87	570.73	0.46	249.15	0.44
RBK Design	299.70	570.73	0.53	281.28	0.49

Table 7
Resulting Unity Checks for different Levels of Approximation for shear, span 2.

	LoA I $v_{Ed,x}$ (kN/m)	$v_{Rd,c}$ (kN/m)	UC	LoA II $v_{Ed,x}$ (kN/m)	UC
RBK Usage	363.90	562.97	0.65	290.13	0.52
RBK Reconstruction	372.51	562.97	0.66	296.89	0.53
RBK Design	419.87	562.97	0.75	334.46	0.59

making strategy is still necessary: looking at the predictions for an on-site test.

6. Multi-level prediction of behavior during field test of Nieuwklap bridge

For the multi-level prediction of the expected behavior in the experiment, all load and resistance factors are taken as equal to 1. Since the capacity using levels 1 and 2 is the same, and a linear finite element model is recommended for the preparation of field tests [4,5], this analysis focuses on the use of the linear finite element model to predict the behavior during the field test. The analyses explore the effect of using different material properties for the steel (as the type of steel in the bridge is unknown), and explore if the bridge would be a good candidate for collapse testing if the asphalt layer is removed.

The resulting bending moment capacity for span 1 is m_u = 864.76 kNm/m and for span 2 m_u = 848.17 kNm/m when f_{cm} = 70 MPa is used. To analyze if shear failure occurs before yielding of the reinforcement steel, the yielding moment is calculated. This value is m_y = 777.69 kNm/m for span 1 and 762.42 kNm/m for span 2. To determine the mean shear capacity, mean material parameters are used in Eq. and $C_{Rd,c}$ = 0.15 is used [21], which results in $v_{R,c}$ = 678.70 kN/m for span 1 and $v_{R,c}$ = 669.47 kN/m for span 2.

To find the maximum load that is expected to cause failure during the test, the load on the design tandem is determined for which the load effect equals the capacity at the section with the largest load effect. Table 8 gives an overview of the results from these calculations. The results identified with “bending moment” and “yielding” are loads for the tandem at the flexure-critical position, where “bending moment” indicates that the ultimate moment is reached in the cross-section, and “yielding” indicates that the yield moment is reached. The results identified with “shear”, “bending moment at 2.5 d_l”, and “yielding at 2.5 d_l” are determined for the tandem at 2.5 d_l from the face of the support. For this position, the maximum load for bending moment and the yielding moment is determined to see if shear failure occurs before yielding of the steel or before flexural failure. For span 1, the results indicate that flexural failure occurs before shear failure. For span 2, shear failure can occur before yielding of the reinforcement steel when the tandem is placed at 2.5 d_l from the face of support 2 (for QR22 steel, we expect shear failure for a load of 2490 kN, which is lower than the load that would cause yielding of the cross-section at that position, 2972 kN and then a bending moment failure at 3330 kN).

Table 8
Overview of results for maximum load that is expected to cause failure in the test. All values in kN.

	Case	QR22	QR24	no asphalt, QR22
span 1	Bending moment	1969	2179	2033
	Yielding	1727	1936	1791
	Shear	3547	3376	3617
	Bending moment at 2.5 d_l	2276	2518	2348
	Yielding at 2.5 d_l	1998	2238	2070
span 2	Bending moment	1844	2042	1906
	Yielding	1614	1809	1677
	Shear	2490	2362	2564
	Bending moment at 2.5 d_l	3330	3640	3362
	Yielding at 2.5 d_l	2972	3276	3003
	Shear at 14.7 m	3400	3323	3479
	Bending moment at 14.7 m	2105	2326	2167
	Yielding at 14.7 m	1850	2066	1912

For span 2, however, the effect of the bent-up bars should be taken into account, see Fig. 12. These bars work as shear reinforcement, and are expected to increase the shear capacity significantly. Therefore, the analysis is also carried out with the tandem outside of the region in which bent-up bars are present, or at 3.5 m from support 2 (14.7 m from support 1). This position reflects the behavior of typical reinforced concrete slab bridges without shear reinforcement. The results from Table 8 show that for this position, flexural failure is expected to occur before shear failure.

The results in Table 8 explore the influence of the reinforcement grade (QR22 or QR24). The maximum load required to cause failure will increase if QR24 steel is present in the bridge, but the steel grade has no influence on the failure mode. The reason why it is important to evaluate the effect of a different reinforcement grade is that the effect of the yield strength of the steel is different for the flexural capacity and the shear capacity. An increase in yield strength of the steel results in an increase in the flexural capacity. For shear, the effect is different, and Eq. shows that the lower bound of the shear capacity is inversely proportional to the yield strength of the steel, so that for higher values of the yield strength of the steel a shear failure mode can govern over the flexural failure mode. For the Nieuwklap bridge, the calculations show that the steel grade does not change the failure mode.

Moreover, the effect of removing the asphalt layer is studied. Since the asphalt layer is a distributed load, removing the asphalt layer will require more concentrated load on the tandem to cause failure, which could potentially change the failure mode. The results in Table 8 show that removing the asphalt layer does not make the bridge more shear-critical.

The linear finite element model can be used to find the load effects that are required input for the Extended Strip Model [99,100], a plasticity-based model that considers the interaction between one-way shear and two-way flexure in slabs under concentrated loads. The experience from the failure testing of the Ruytenschildt Bridge teaches us that this model gives a good prediction of the maximum load required to cause failure [101], with about 20% conservativism. With the Extended Strip Model, the value for the maximum load on span 1 becomes 4459 kN and 5390 kN for span 2. Taking into account the 20% conservativism results in a required load of 6468 kN. Applying such large loads in a field test complicates the execution of the test and may endanger the safety of the executing personnel. The reason why these loads are significantly larger than the loads predicted in Table 8 is because the redistribution capacity of reinforced concrete slabs is large, which results in higher capacities than predicted with a Level II approach. However, the Level II approach is suitable for evaluating if the Nieuwklap bridge is a suitable candidate for a collapse test in shear. Both the results of the multi-level assessment and the multi-level prediction approach show that the Nieuwklap bridge is a flexure-critical structure and that a collapse test will not give insight in the shear behavior of reinforced concrete slab bridges.

7. Discussion

Comparing the results of the two Levels of Approximation shows that for both approaches (multi-level assessment and multi-level prediction of behaviour), the linear finite element model gives a more accurate assessment and predicted. This observation is reflected by the lower Unity Checks when using the linear finite element model approach. Both approaches also indicated that the Nieuwklap bridge is not shear-critical and that the objectives of the test could not be met.

Since both Levels of Approximation I and II already clearly showed that the test objectives could not be met, the third and final Level of Approximation was not used. For structures of which the behaviour is not captured well by typical design expressions, such as shear-critical reinforced concrete slabs which can exhibit large amounts of transverse redistribution, as well as for slab bridges with a large skew angle, 3D NLFEA can be recommended to predict the required load in a field test and to predict the failure mode. Such analyses have been carried out successfully in the past [38,62,102]. However, 3D NLFEA are time-consuming and complex. Therefore, it is recommended to combine these calculations with simpler linear elastic finite element models and hand calculations, and to first evaluate if the simpler approaches can already give sufficient insight in the feasibility of the test.

The novelty of the proposed decision-making strategy is that it shows that two paths of calculations are necessary for the preparation of a field test: the assessment calculations, as well as prediction calculations. Assessment calculations may be available, and may be the initial driving factor to decide to load test a bridge. However, the prediction calculations are necessary as well. The assessment calculations are based on the live load model that is used in the code, consisting of a distributed lane load and (for the Eurocode) a tandem of concentrated loads in each lane. For proof and collapse load tests, this complex load model is often simplified into a single tandem load. The result is that the concentration of the loads increases, which may favor shear failure modes over flexural failure modes. Therefore, the prediction calculations, that focus on finding the maximum tandem load to cause failure, should be added to the preparation stages of proof and collapse load tests.

The proposed framework in this article describes the preparation of a test that serves one specific goal. If the test would serve multiple objectives, then the flowchart of Fig. 2 and its associated charts in Fig. 3 and Fig. 4 should be extended in such a way that all objectives of the test are addressed and evaluated. If different test objectives would result in conflicting recommendations in terms of the cost-benefit or execution of the test, a consensus should be reached with the bridge owner in a discussion on the feasibility of the test and its various objectives.

The case of the Nieuwklap bridge presents a few interesting vintage details, as the bridge was designed in the 1930 s. The hooks on the reinforcement makes that this bridge has a higher shear resistance than the typical shear-critical slab bridges from the 1960 s that are present in the Netherlands [17,70]. For the analysis of the Nieuwklap bridge, we focused on the reinforced concrete slab. The sidewalk, which had a larger stiffness because of its cross-section, and which included stirrups in the edge beam, results in larger transverse redistribution. The original plan for the collapse test would have been to provide a saw cut between the slab and the sidewalk, to eliminate the beneficial effect of the sidewalk. However, analyzing only the slab indicated that the structure was not shear-critical.

The Nieuwklap bridge has a skew angle of 8°. From the linear finite element analyses, it is clear that this small skew angle does not have a significant effect on the overall behavior. For reinforced concrete slab bridges with skew angles of 15° and larger, the skew results in a concentration of stresses in the obtuse corner [103,104] as well as a redistribution of bending moment between the longitudinal and transverse reinforcement [105].

Some uncertainties on the proposed approach relate to the model for shear capacity used currently for assessment. Topics that require further study to improve the shear capacity expressions are the influence of the size effect in shear [24,106–109] and the effect of plain bars on the shear resistance [110–112]. These topics are currently being addressed with experimental studies, which will improve our understanding of shear capacity and will allow us to propose improved formulations for the shear capacity that then can be embedded in this multi-level decision strategy.

Drawing from the experience of previous collapse testing in the Netherlands [14,54], we identified that a careful preparation of a potential collapse test on the Nieuwklap bridge was necessary. From the collapse test on the Ruytenschildt bridge, we learned that achieving a shear failure on a reinforced concrete slab bridge may be difficult on site, and that the failure mode should be carefully studied prior to the test. In an analysis of the bridge after the test, we found that, taking into account the considerations discussed in this article, a shear failure would not have been likely [49,50]. From the collapse test on the Vecht Bridge [54], we learned that sufficient time on site for carrying out all prepared experiments may be a limiting factor, and that a careful planning of the on-site activities is key to a smooth execution in the field. For this case study, we carried out preliminary calculations on the capacity and failure mode that are in line with what is described in this article, but in a more succinct manner because of the lack of time. These lessons learned inspired the initial feasibility study for a potential collapse test on the Nieuwklap bridge, and resulted in an informed decision to not load test the bridge.

8. Recommendations for practice

Previous work on bridge load testing has emphasized the importance of a good preparation of the load test to properly evaluate if the test objectives can be met [1,4]. However, guidance on how to carry out the preparations for a proof load test or a collapse test is often not detailed in terms of which preparatory calculations should be carried out. This study proposes a multi-level assessment and prediction strategy that can be used in the decision-making process for a load test, as shown in the flowcharts Fig. 2, Fig. 3, and Fig. 4. This standardized approach can be followed to evaluate if a field test can meet the identified goals, and if the test engineers should proceed with planning and preparing the test. For general load tests, this approach can be used to evaluate if a load test is recommended for the evaluation of a given bridge. All levels of assessment and predictions may be recommended for the preparation of proof load tests when the uncertainties on the expected behavior are large. For failure tests, this approach can be used to evaluate if the failure test can meet the goals stipulated for the test, and to determine if the bridge under study is a good candidate for a failure test. Moreover, the decision-making approach includes as well guidance on which steps follow in the preparation after the calculation steps, and puts emphasis on evaluating safety during the experiment and the site conditions.

Based on the flowchart in Fig. 2, we can recommend the following steps for the preparation of load tests:

- Gather all required information about the bridge: design calculations, design and as-built plans, results of material testing, reports about changes to the bridge (if any), inspection reports, assessment reports.
- Carry out a multi-level assessment of the structure to find the Unity Checks, see Fig. 3.
- Carry out a multi-level prediction of the maximum load on the tandem during the test to find the governing failure mode and, in case of a collapse test, lower bound of the required load to cause collapse, see Fig. 4.
- Evaluate the assessment and prediction calculations to see if the field test can meet the stipulated goals.
- Determine the load application method and loading protocol, as well as the sensor plan.
- Evaluate if the prepared load application method and loading protocol, as well as the sensor plan are possible under the site conditions.
- Evaluate if there are no major risks to the personnel and/or travelling public.
- Develop the planning of the on-site activities.

9. Summary and conclusions

Careful preparations are essential for load tests. For proof load tests and failure tests, the large magnitudes of loads involved in the test make this even more important. In this paper, we present a multi-level decision-making approach for load tests, especially proof and collapse load tests. The goal of the multi-level decision-making approach is to identify if the objectives of the proposed test can be met. The novelty of the proposed method lies in a combination of the assessment calculations that are typically carried out with prediction calculations that aim at better understanding the actual conditions during the load test. Both approaches are proposed as several Levels of Approximation.

The proposed decision strategy was applied to the case of the Nieuwklap bridge, which was available for a collapse test prior to its demolition and replacement. The objective of the test was to cause a shear failure in span 1 and/or span 2. Following the multi-level decision-making strategy, it was found that this bridge from the 1930 s is not representative of the typical shear-critical slab bridges in the Netherlands and that the test objective could not be met. As such, using the multi-level decision-making strategy resulted in an informed decision to not continue with the preparation of the test, as the benefit of this test and information that could be obtained from the test would not justify its cost.

CRediT authorship contribution statement

Eva Olivia Leontien Lantsoght: Conceptualization, Methodology, Software, Formal analysis, Investigation, Data curation, Writing – original draft, Visualization. **Yuguang Yang:** Methodology, Validation, Investigation, Writing – review & editing. **Cor van der Veen:** Conceptualization, Methodology, Validation, Investigation, Resources, Supervision, Project administration, Funding acquisition.

Declaration of Competing Interest

The authors declare that they have no known competing financial interests or personal relationships that could have appeared to influence the work reported in this paper.

Acknowledgement

The authors wish to express their gratitude and sincere appreciation to the province Groningen for financing this research work. We are grateful for the contributions of MSc thesis student Marios Tzortzinakis and exchange PhD candidate Tomas Agustin who carried out additional calculations for the preparation of the test. We also value the input of our former colleague Dick Hordijk on the load testing research and decision-making strategy.

References

[1] Lantsoght EOL, van der Veen C, de Boer A, Hordijk DA. State-of-the-art on load testing of concrete bridges. Eng Struct 2017;150:231–41.
[2] Bonifaz J, Zaruma S, Robalino A, Sanchez TA. Bridge Diagnostic Load Testing in Ecuador – Case Studies. IALCCE 2018. Ghent, Belgium2018.
[3] Sanayei M, Reiff AJ, Brenner BR, Imbaro GR. Load Rating of a Fully Instrumented Bridge: Comparison of LRFR Approaches. J Perform Constr Facil 2016;30(2): 04015019. https://doi.org/10.1061/(ASCE)CF.1943-5509.0000752.
[4] Alampalli S, Frangopol DM, Grimson J, Halling MW, Kosnik DE, Lantsoght EOL, et al. Bridge Load Testing: State-of-the-Practice. J Bridge Eng 2021;26(3): 03120002. https://doi.org/10.1061/(ASCE)BE.1943-5592.0001678.
[5] Alampalli S, Frangopol DM, Grimson J, Kosnik D, Halling M, Lantsoght EOL, et al. Primer Bridge Load Testing. 2019:136.
[6] Halicka A, Hordijk DA, Lantsoght EOL. Rating of concrete road bridges with proof loads. ACI SP 323 Evaluation Concrete Bridge Behavior through Load Testing – Int Perspect 2018;16.
[7] Lantsoght EOL, Van der Veen C, De Boer A, Hordijk DA. Assessment of slab bridges through proof loading in the Netherlands. ACI SP Evaluation of Concrete Bridge Behavior through Load Testing – Int Perspect 2018.
[8] Bagge N, Popescu C, Elfgren L. Failure tests on concrete bridges: Have we learnt the lessons? Struct Infrastruct Eng 2018;14(3):292–319.
[9] Ensink SWH, Van der Veen C, Hordijk DA, Lantsoght EOL, van der Ham H, De Boer A. Full-size field test of prestressed concrete T-beam bridge. European Bridge Conference. Edinburgh, Scotland2018.
[10] Lantsoght EOL, Yang Y, van der Veen C, de Boer A, Hordijk DA. Ruytenschildt Bridge: field and laboratory testing. Eng Struct 2016;128:111–23.
[11] Huber P, Vill M, Schweighofer A, Kollegger J. Full-scale shear tests on post-tensioned bridge girders of existing bridges. Structural Concrete 2018;19:5–15.
[12] Lantsoght EOL, Zarate G, Zhang F, Yang Y, Park M, Sliedrecht H. Shear experiments of prestressed concrete bridge girders. ACI Struct J 2021;118: 117–30.
[13] Zhang F, Zarate Garnica GI, Yang Y, Lantsoght E, Sliedrecht H. Monitoring Shear Behavior of Prestressed Concrete Bridge Girders Using Acoustic Emission and Digital Image Correlation. Sensors. 2020;20(19):5622. https://doi.org/10.3390/s20195622.
[14] Lantsoght E, van der Veen C, de Boer A, Hordijk D. Collapse test and moment capacity of the Ruytenschildt Reinforced Concrete Slab Bridge Structure Infrastructure Eng 2017;13(9):1130–45.
[15] Halding PS, Schmidt JW, Jensen TW, Henriksen AH. Structural response of full-scale concrete bridges subjected to high load magnitudes. SMAR 2017 - 4th conference on smart monitoring, assessment and rehabilitation of civil structures2017.
[16] Schmidt JW, Halding PS, Jensen TW, Engelund S. High Magnitude Loading of Concrete Bridges. Special Publication 2018;323.
[17] Lantsoght EOL, van der Veen C, Walraven J, de Boer A. Recommendations for the Shear Assessment of Reinforced Concrete Slab Bridges from Experiments Structural Eng Int 2013;23(4):418–26.
[18] Walraven JC. Residual shear bearing capacity of existing bridges. fib Bulletin 57, Shear and punching shear in RC and FRC elements; Proceedings of a workshop held on 15-16 October 2010. Salò, Lake Garda, Italy2010. p. 129-38.
[19] Eurocode CEN. 2: Design of Concrete Structures - Part 1–1 General Rules and Rules for Buildings. Brussels, Belgium: Comité Européen de Normalisation; 2005. p. 229.
[20] König G, Fischer J. Model Uncertainties concerning Design Equations for the Shear Capacity of Concrete Members without Shear Reinforcement. CEB Bulletin 224, Model Uncertainties and Concrete Barrier for. Environmental Protection. 1995:49–100.
[21] Regan PE. Enhancement of shear resistance in short shear spans of reinforced concrete - an evaluation of UK reccomendations and particularly of BD44/95. London, UK: University of Westminster; 1998. p. 16.
[22] Reineck K-H, Bentz EC, Fitik B, Kuchma DA, Bayrak O. ACI-DAfStb Database of Shear Tests on Slender Reinforced Concrete Beams without Stirrups. ACI Struct J 2013;110:867–76.
[23] Lantsoght EOL, van der Veen C, de Boer A, Walraven J. Transverse Load Redistribution and Effective Shear Width in Reinforced Concrete Slabs. Heron. 2015;60:145–80.
[24] Yang Y. Shear Capacity of RC Slab Structures with Low Reinforcement Ratio - an Experimental Approach. fib symposium 2021. Lisbon (online)2021.
[25] Sykora M, Krejsa J, Mlcoch J, Prieto M, Tanner P. Uncertainty in shear resistance models of reinforced concrete beams according to fib MC2010. Structural Concrete. 2018;19:284–95.
[26] Haritos N, Hira A, Mendis P, Heywood R, Giufre A. Load testing to collapse limit state of Barr Creek Bridge. Fifth International Bridge Engineering Conference, Vols 1 and 2: Bridges, Other Structures, and Hydraulics and Hydrology2000. p. A92-A102.
[27] Azizinamini A, Boothby TE, Shekar Y, Barnhill G. Old Concrete Slab Bridges. 1. Experimental Investigation. J Structural Eng-ASCE 1994;120:3284–304.
[28] Azizinamini A, Shekar Y, Boothby TE, Barnhill G. Old concrete slab bridges. 2: Analysis. J Structural Eng-ASCE. 1994;120:3305–19.
[29] Miller RA, Aktan AE, Shahrooz BM. Destructive testing of decommisisioned concrete slab bridge. J Structural Eng-Asce. 1994;120:2176–98.
[30] Aktan AE, Zwick M, Miller R, Shahrooz B. Nondestructive and Destructive Testing of Decommissioned Reinforced Concrete Slab Highway Bridge and Associated Analytical Studies. Transportation Research Record: J Transportation Research Board. 1992;1371:142–53.
[31] Jorgenson JL, Larson W. Field Testing of a Reinforced Concrete Highway Bridge to Collapse. Transportation Research Record: J Transportation Research Board 1976;607:66–71.
[32] Steinberg E, Miller R, Nims D, Nims D. Structural Evaluation of LIC-310-0396 and FAY-35-17-6.82 Box Beams with Advanced Strand Deterioration. Athens, Ohio2011. p. 131.
[33] Puurula A, Enochsson O, Sas G, Blanksvard T, Ohlsson U, Bernspang L, et al. Challenges in Design and Construction of an Innovative and Sustainable Built Environment. Stockholm 2016;2016:2526–33.
[34] Nilimaa J, Bagge N, Blanksvärd T, Täljsten B. NSM CFRP Strengthening and Failure Loading of a Posttensioned Concrete Bridge. J Compos Constr 2016;20(3): 04015076. https://doi.org/10.1061/(ASCE)CC.1943-5614.0000635.
[35] Nilimaa J, Nilforoush R, Bagge N, Elfgren L. Testing to Failure of a 55-year-old Prestressed Concrete Bridge in Kiruna : Bending, Shear and Punching of Girders and Slab. Fracture Properties of Materials. Test Results, Modelling and Assessment. Final Report BBT 2017-030. Forskningsrapport / Luleå tekniska universitet. Luleå: Luleå University of Technology; 2020. p. 77.
[36] Puurula AM, Enochsson O, Sas G, Blanksvärd T, Ohlsson U, Bernspång L, et al. Assessment of the Strengthening of an RC Railway Bridge with CFRP Utilizing a Full-Scale Failure Test and Finite-Element Analysis. J Struct Eng 2015;141(1). https://doi.org/10.1061/(ASCE)ST.1943-541X.0001116.
[37] Ferreira D, Bairán J, Marí A. Efficient 1D model for blind assessment of existing bridges: simulation of a full-scale loading test and comparison with higher order continuum models. Struct Infrastruct Eng 2015;11(10):1383–97.
[38] Puurula AM, Enochsson O, Sas G, Blanksvärd T, Ohlsson U, Bernspång L, et al. Loading to failure and 3D nonlinear FE modelling of a strengthened RC bridge. Struct Infrastruct Eng 2014;10(12):1606–19.
[39] Elfgren L. Discussion of "Failure Load Test of a CFRP Strengthened Railway Bridge in Örnsköldsvik, Sweden" by Marcus Bergström, Björn Täljsten, and Anders Carolin. J Bridge Eng. 2011;16:490-.
[40] Bergström M, Täljsten B, Carolin A. Failure Load Test of a CFRP Strengthened Railway Bridge in Örnsköldsvik Sweden. J Bridge Eng 2009;14(5):300–8.

[41] Wang FM, Kang SZ, Cai YC, Li XL. Destructive Test Study of A Prestressed Concrete Hollow Slab Beam Bridge. Geotech Special Publ No 214 - Am Soc Civil Eng 2011:57–64.
[42] Zhang J, Peng H, Cai CS. Destructive Testing of a Decommissioned Reinforced Concrete Bridge. J Bridge Eng 2013;18(6):564–9.
[43] Zhang J, Peng H, Cai CS. Field Study of Overload Behavior of an Existing Reinforced Concrete Bridge under Simulated Vehicle Loads. J Bridge Eng 2011;16 (2):226–37.
[44] Zhang J-r, Peng H, Zhang K-b, Hao H-x. Test Study on Overload and Ultimate Behavior of Old Reinforced Concrete Bridge Through Destructive Test of Corroded Bridge. Eng Mech 2009;26:213–24.
[45] Bakht B, Jaeger LG. Ultimate Load Test of Slab-on-Girder Bridge. J Struct Eng 1992;118(6):1608–24.
[46] Jiaquan X, Zanping W, Bing H, Guanhua F, Yufeng Z, Jianfei Z. Practical experimental study on ultimate bearing capacity of actual bridge in Huning Expressway Extension project. Modern Transportation Technol 2006;5:77–84.
[47] Lantsoght E. Measurements of Ruytenschildt Bridge test and analysis for stop criteria. Delft University Technology 2017:60.
[48] Lantsoght EOL. Beams from Ruytenschildt Bridge: Analysis of stop criteria. Delft University Technology 2017:77.
[49] Lantsoght E, van der Veen C, de Boer A. Shear and moment capacity of the Ruytenschildt bridge. IABMAS 20162016. p. 8.
[50] Lantsoght EOL, van der Veen C, de Boer A, Hordijk DA. Probabilistic prediction of the failure mode of the Ruytenschildt Bridge. Eng Struct 2016;127:549–58.
[51] Lantsoght EOL. Ruytenschildt Bridge: analysis of test results at the ultimate limit state (in Dutch). Delft, The Netherlands: Delft University of Technology; 2015. p. 89.
[52] Yang Y. Experimental Studies on the Structural Behaviours of Beams from Ruytenschildt Bridge. Delft University of Technology; 2015.
[53] Lantsoght EOL. Ruytenschildt Bridge: Preparation of test to failure in span of slab (in Dutch). Delft, The Netherlands: Delft University of Technology; 2014. p. 74.
[54] Koekkoek RT. Measurement Report Loading of Vechtbrug 2017;25H–100:55.
[55] Gehrlein S, Landler J, Oberndorfer T, Fischer O. In-Situ Shear TEstson a 64-year-old Road Bridge. fib 2018. Melbourne, Australia2018.
[56] Gehrlein S, Landler J, Oberndorfer T, Fischer O. Großversuche zur Querkrafttragfähigkeit bestehender Spannbetonbrücken an der Saalebrücke Hammelburg. Beton- Stahlbetonbau 2018;113(9):667–75.
[57] Gehrlein S, Fischer O. Großversuche zur Querkrafttragfähigkeit bestehender Spannbetonbrücken an der Saalebrücke Hammelburg. Beton- Stahlbetonbau 2018;113(10):696–704.
[58] Gehrlein S, Landler J, Oberndorfer T, Fischer O. Querkraftversuche an der Saalebrücke Hammelburg. Tagungsband zum 21 Münchener Massivbau Seminar 2017.
[59] Lantsoght E, de Boer A, van der Veen C. Levels of Approximation for the shear assessment of reinforced concrete slab bridges. Structural Concr 2017;18(1): 143–52.
[60] fib. Model code 2010: final draft. Lausanne: International Federation for Structural Concrete; 2012.
[61] Shu J, Plos M, Zandi K, Lundgren K. A Multi-level Structural Assessment Proposal for Reinforced Concrete Bridge Deck Slabs. Nordic Concrete Res 2015:53–6.
[62] Shu Jiangpeng, Bagge Niklas, Plos Mario, Johansson Morgan, Yang Yuguang, Zandi Kamyab. Shear Capacity of a RC Bridge Deck Slab: Comparison between Multilevel Assessment and Field Test. J Struct Eng 2018;144(7):04018081. https://doi.org/10.1061/(ASCE)ST.1943-541X.0002076.
[63] Cremona Christian, Poulin Benoît. Standard and advanced practices in the assessment of existing bridges. Struct Infrastruct Eng 2017;13(4):428–39.
[64] Brühwiler Eugen, Vogel Thomas, Lang Thomas, Lüchinger Paul. Swiss Standards for Existing Structures. Struct Eng Int 2012;22(2):275–80.
[65] Muttoni Aurelio, Ruiz Miguel Fernández. Levels-of-Approximation Approach in Codes of Practice. Struct Eng Int 2012;22(2):190–4.
[66] Bundesministerium für Verkehr Bau und Stadtentwicklung - Abteilung Straßenbau. Richtlinie zur Nachrechnung von Straßenbrücken im Bestand (Nachrechnungsrichtlinie). 2011. p. 108.
[67] Marzahn Gero. Zur Richtlinie für die Nachrechnung von Straßenbrücken im Bestand (Nachrechnungsrichtlinie). Beton- Stahlbetonbau 2011;106(11):730–5.
[68] Bagge Niklas. Demonstration and examination of a procedure for successively improved structural assessment of concrete bridges. Structural Concr 2020;21(4): 1321–44.
[69] Frangopol DM, Sabatino S, Dong Y. Bridge Life-Cycle Performance and Cost: Analysis, Prediction, Optimization and Decision Making. In: Bittencourt, Frangopol, Beck, editors. Maintenance, Monitoring, Safety, Risk and Resilience of Bridges and Bridge Networks. Foz do Iguacu, Brazil2016. p. 2-20.
[70] Lantsoght Eva OL, van der Veen Cor, Hordijk Dick A, de Boer Ane. Development of recommendations for proof load testing of reinforced concrete slab bridges. Eng Struct 2017;152:202–10.
[71] Code Committee 351001. Assessement of structural safety of an existing structure at repair or unfit for use - Basic Requirements, *NEN 8700:2011* (in Dutch). Delft, The Netherlands: Civil center for the execution of research and standard, Dutch Normalisation Institute; 2011.
[72] Rijkswaterstaat. Guidelines Assessment Bridges - assessment of structural safety of an existing bridge at reconstruction, usage and disapproval (in Dutch), RTD 1006:2013 1.1. Utrecht, the Netherlands2013. p. 117.
[73] Blomfors M, Engen M, Plos M. Evaluation of safety formats for non-linear finite element analyses of statically indeterminate concrete structures subjected to different load paths. Structural Concrete. 2016;17:44-51.
[74] Belletti Beatrice, Pimentel Mário, Scolari Matteo, Walraven Joost C. Safety assessment of punching shear failure according to the level of approximation approach. Structural Concr 2015;16(3):366–80.
[75] Caspeele Robby, Sykora Miroslav, Allaix Diego Lorenzo, Steenbergen Raphaël. The Design Value Method and Adjusted Partial Factor Approach for Existing Structures. Struct Eng Int 2013;23(4):386–93.
[76] Code Committee 351001. Eurocode 1 - Actions on structures - Part 2: Traffic loads on bridges, EN 1991-2/NA:2011. Delft, The Netherlands: Civil engineering center for research and regulation, Dutch Normalization Institute; 2011. p. 38.
[77] Lantsoght EOL, van der Veen C, Walraven JC. Shear in One-way Slabs under a Concentrated Load close to the support. ACI Struct J 2013;110:275–84.
[78] Huber Patrick, Huber Tobias, Kollegger Johann. Influence of loading conditions on the shear capacity of post-tensioned beams with low shear reinforcement ratios. Eng Struct 2018;170:91–102.
[79] de Jong W. Object: VB035 - Brug Nieuwklap. IASSET 2015.
[80] Gijsbers FBJ, Steenbergen RDJM, Cvd Veen. Werkset factoren plaatconstructies van gewpaend beton zonder dwarskrachtwapening. TNO / TU Delft 2011:24.
[81] Yang Y, Den Uijl JA, Dieteren G, de Boer A. Shear capacity of 50 years old reinforced cocnrete bridge deck without shear reinforcement. 3rd fib International Congress. Washington DC, USA: fib; 2010. p. 12.
[82] Rijkswaterstaat. Richtlijnen Beoordeling Kunstwerken - beoordeling van de constructieve veiligheid van een bestaand kunstwerk bij verbouw, gebruik en afkeur. RTD 1006:20132013. p. 117.
[83] Lantsoght EOL. Bezwijktest Nieuwklapbrug: voorbereidingsrapport. 2018. p. 127.
[84] Lantsoght EOL, Van der Veen C, Walraven J, De Boer A. Applying Experimental Results to the Shear Assessment Method for Solid Slab Bridges. Concrete 2013. Gold Coast, Australia2013. p. 10 pp.
[85] Lantsoght EOL, van der Veen C, De Boer A, Walraven J. Influence of Width on Shear Capacity of Reinforced Concrete Members. ACI Struct J 2014;111:1441–50.
[86] Scia Nemetschek. Scia helpfile release 2018;17:1.
[87] Cope RJ, Rao PV. SHEAR FORCES IN EDGE ZONES OF CONCRETE SLABS. Structural Eng 1984;62:87–92.
[88] Cope RJ. Flexural Shear Failure of Reinforced-Concrete Slab Bridges. Proceedings of the Institution of Civil Engineers Part 2-Research and Theory. 1985;79:559-83.
[89] Eurocode CEN. 1: Actions on structures - Part 2: Traffic loads on bridges. Brussels, Belgium: Comité Européen de Normalisation; 2003. p. 168.
[90] Lantsoght EOL, van der Veen C, de Boer A, Walraven J. Using Eurocodes and AASHTO for assessing shear in slab bridges. Proceedings of the Institution of Civil Engineers – Bridge Engineering. 2016;169:285-97.
[91] Vergoossen R, Naaktgeboren M, ‘t Hart M, De Boer A, Van Vugt E. Quick Scan on Shear in Existing Slab Type Viaducts. International IABSE Conference, Assessment, Upgrading and Refurbishment of Infrastructures. Rotterdam, The Netherlands2013. p. 8.
[92] Lantsoght Eva, van der Veen Cor, de Boer Ane, Hordijk Dick A. Proof load testing of reinforced concrete slab bridges in the Netherlands. Structural Concr 2017;18 (4):597–606.
[93] Rijkswaterstaat. Quick Scan Platen 2012 - Modelbeschrijving. 2013. p. 51.
[94] Lantsoght EOL, van der Veen C, Gijsbers FBJ. Background report for spreadsheet for checks at the edge. Delft University of Technology; 2012. p. 50.
[95] Walraven JC. Minimum shear capacity of reinforced concrete slabs without shear reinforcement: the value v_{min}. 2013. p. 20 (in Dutch).
[96] Steenbergen RDJM, Vervuurt AHJM. Determining the in situ concrete strength of existing structures for assessing their structural safety. Structural Concrete. 2012; 13(1):27–31.
[97] Koekkoek RT, Lantsoght EOL, Yang Y, Hordijk DA. Analysis report for the assessment of Viaduct De Beek by Proof Loading. Delft, The Netherlands: Delft University of Technology; 2016. p. 125.
[98] Lantsoght Eva OL, de Boer Ane, van der Veen Cor. Distribution of peak shear stress in finite element models of reinforced concrete slabs. Eng Struct 2017;148: 571–83.
[99] Lantsoght EOL, van der Veen C, de Boer A, Alexander SDB. Extended Strip Model for Slabs under Concentrated Loads. ACI Struct J 2017;114:565–74.
[100] Lantsoght Eva OL, van der Veen Cor, de Boer Ane. Extended Strip Model for slabs subjected to load combinations. Eng Struct 2017;145:60–9.
[101] Lantsoght EOL, van der Veen C, de Boer A, Alexander S. Bridging the gap between one-way and two-way shear in slabs. ACI-fib international symposium: Punching shear of structural concrete slabs; 2017. p. 187–214.
[102] Lantsoght EOL, de Boer A, van der Veen C, Hordijk DA. Optimizing Finite Element Models for Concrete Bridge Assessment With Proof Load Testing. Frontiers. Built Environ 2019;5.
[103] Cope RJ, Clark LA. Concrete slabs : analysis and design. London: Elsevier Applied Science; 1984.
[104] Cope RJ, Rao PV, Edwards KR. Shear in skew reinforced concrete slab bridges – analytical and experimental studies – A report to the Department of Transport. Liverpool, UK: University of Liverpool; 1983. p. 219.
[105] Moya L, Lantsoght EOL. Parametric Study on the Applicability of AASHTO LRFD for Simply Supported Reinforced Concrete Skewed Slab Bridges. Infrastructures. 2021;6:88.
[106] Bazant ZP, Kim JK. Size Effect in Shear Failure of Longitudinally Reinforced Beams. J Am Concrete Inst 1984;81:456–68.
[107] Shioya T, Iguro M, Nojiri Y, Akiyama H, Okada T. Shear strength of large reinforced concrete beams. Fracture Mechanics: Application to Concrete. 1989; ACI SP-118:259-79.
[108] Bazant ZP, Kazemi MT. Size effect on Diagonal Shear Failure of Beams without Stirrups. ACI Struct J 1991;88:268–76.

[109] Walraven J, Lehwalter N. Size Effects in Short Beams Loaded in Shear. ACI Struct J 1994;91:585–93.

[110] Feldman LR, Bartlett FM. Bond in flexural members with plain steel reinforcement. ACI Struct J 2008;105:552–60.

[111] Lantsoght Eva OL, van der Veen Cor, Walraven Joost, de Boer Ane. Experimental investigation on shear capacity of reinforced concrete slabs with plain bars and slabs on elastomeric bearings. Eng Struct 2015;103:1–14.

[112] Yang Y, van der Veen C, Hordijk D, De Boer A. The shear capacity of reinforced concrete members with plain bars. In: Forde M, editor. Structural Faults and Repair 2016. Edinburgh, 20162016. p. 9.